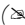




A theoretical framework for radial mass–energy density variations in geophysical systems

Branko M. Novakovic¹ 
Josip Kasac² 



( Corresponding Author)

^{1,2}University of Zagreb, Faculty of Mechanical Engineering and Naval Architecture, Croatia.

¹Email: branko.novakovic@fsb.unizg.hr

²Email: josip.kasac@fsb.unizg.hr

Abstract

This paper introduces a theoretical framework for describing energy-density variations within the Earth using the Relativistic Radial Density Theory (RRDT). The proposed approach models the Earth as a radially structured system in which spatial variations of mass–energy density are linked to underlying geophysical processes. Starting from fundamental physical quantities, including Planck-scale parameters, a set of analytical relations is derived to describe the distribution of radial mass density and its potential temporal evolution. The framework further explores how localized perturbations in radial density fields may be associated with changes in the dynamical state of the lithosphere. In this context, a conceptual measurement scheme is outlined, combining conventional sensing (e.g., seismometers) with distributed or mobile platforms for multi-scale data acquisition. The presented model is intended as a hypothesis-generating theoretical construct rather than a validated predictive tool. Its purpose is to provide a formal basis for future investigations of energy-density anomalies in geophysical systems and to suggest directions for experimental validation and interdisciplinary research. Potential implications for seismic hazard assessment are discussed at a conceptual level.

Keywords: Artificial intelligence, Geophysical systems, Early prediction, Earthquakes, Measurement by robots, Radial mass density theory.

Citation | Novakovic, B. M., & Kasac, J. (2026). A theoretical framework for radial mass–energy density variations in geophysical systems. *International Review of Applied Sciences*, 12(1), 10–16. 10.20448/iras.v12i1.8703

History:


Received: 7 April 2026

Revised: 12 May 2026

Accepted: 18 May 2026

Published: 22 May 2026

Licensed: This work is licensed under a [Creative Commons](https://creativecommons.org/licenses/by/4.0/)

Attribution 4.0 License 

Publisher: Asian Online Journal Publishing Group

Funding: This study received no specific financial support.

Institutional Review Board Statement: Not applicable.

Transparency: The authors confirm that the manuscript is an honest, accurate, and transparent account of the study; that no vital features of the study have been omitted; and that any discrepancies from the study as planned have been explained. This study followed all ethical practices during writing.

Competing Interests: The authors declare that they have no competing interests.

Authors' Contributions: Both authors contributed equally to the conception and design of the study. Both authors have read and agreed to the published version of the manuscript.

Contents

1. Introduction	11
2. Dynamics of Earthquakes in Radial Mass Density Theory	12
3. Conclusion	15
References	15

Contribution of this paper to the literature

This paper introduces a novel theoretical framework for describing radial mass–energy density variations in geophysical systems. Unlike conventional earthquake studies, the proposed approach links seismic processes with analytically defined radial density fields and outlines a conceptual multi-scale sensing framework for their potential measurement and future validation.

1. Introduction

As is well known, an earthquake is the consequence of a sudden release of energy in the Earth's lithosphere that creates seismic waves. An earthquake warning system, or earthquake alarm system, is a system of accelerometers, seismometers, communication networks, computers, and alarms designed to notify adjoining regions of a substantial earthquake while it is still in progress. In this sense, a new approach to earthquake prediction is presented here, based on the measurement of radial mass density values on the Earth's radial scale. The maximal radial mass density is located at the Earth's center, whereas the minimal radial mass density is located at the Earth's surface. Changes in this density may occur hours or even months before an earthquake occurs.

Most earthquakes may be very large, such as the Oklahoma earthquake that occurred in 2011 with a magnitude of 5.7 [1]. This earthquake was caused by the disposal of wastewater from oil production into an injection well. In Okuwaki, et al. [2] a seismological analysis of the two earthquakes that devastated Turkey is presented. Furthermore, tectonic earthquakes can occur anywhere where sufficient elastic strain energy has accumulated. This energy drives fracture propagation along a fault plane. In order to warn people effectively, future earthquakes may potentially be predicted through measurements performed on the Earth's surface. In this sense, earthquake prediction software has been developed [3] together with improvements in its performance. Such software should provide short-term earthquake predictions and should also enable measurements sufficiently in advance of future earthquake events. In this context, decreases in pressure and temperature may be measured. By using these measurement techniques in Japan, approximately 70.5% prediction accuracy within one month has been reported.

In Shiraishi [3] seismic nowcasting, using the count of small earthquakes as proxy data to estimate the current dynamical state of seismic activity, is also discussed. As a result, an earthquake potential score is obtained that characterizes the current stage of a defined geographic region within its nominal earthquake cycle. The count of small earthquakes is referred to as “natural time.” In addition to natural time, earthquake sequences can also be analyzed using Shannon information entropy. As a first step toward incorporating seismic information entropy into the nowcasting method, magnitude information may be integrated into natural-time counts using event self-information.

It is well known that an earthquake warning system consists of accelerometers, seismometers, communication systems, computers, and alarms. Therefore, the use of mobile robots may reduce the number of required instruments. Furthermore, it is particularly important to develop a system for the very early prediction of future earthquakes. In this sense, an innovative approach for the prediction of future earthquakes is presented here.

Measurements of wave-induced attenuation in saturated metapelite and the band-limitation of low-frequency earthquakes are discussed in Flidner and French [4]. A unified solid-state theory for pre-earthquake signals is presented in Freund [5]. Furthermore, an alternative source model for very low-frequency events and a granular jamming model for low-frequency earthquakes are discussed [6].

A rapid report on seismic damage to hospitals during the 2023 Turkey earthquake sequence is presented in Qu, et al. [7]. The impacts of water and stress transfer from the ground surface on the shallow earthquake of 11 November 2019 at Le Teil, France, are discussed in Burnol, et al. [8]. A statistical analysis of the variability minima of the order parameter of seismicity using event coincidence analysis is presented in Christopoulos, et al. [9].

This is followed by a discussion of moment-duration scaling of low-frequency earthquakes in Guerrero, Mexico [10]. Seismic electric signals (SES) associated with earthquakes are discussed in Helman [11]. The first widely used method for earthquake measurement was the *Richter scale* (developed by Richter [12]). This scale was based on the amplitude of the largest wave recorded by a specific type of seismometer and the distance between the earthquake and the seismometer. Another method for measuring earthquake strength involves observations by people who experienced the earthquake, together with the amount of resulting damage, in order to estimate earthquake intensity. The Mercalli scale was designed for this purpose. The original scale was introduced by Mercalli [13] and later modified by Wood and Neumann [14] resulting in the *Modified Mercalli Intensity Scale (MMI)*. This scale is particularly useful for understanding the damage caused by large earthquakes. To introduce a new method for the very early prediction of earthquakes, the present study applies the Relativistic Radial Density Theory (RRDT) [15]. In this approach, the main idea is based on the precise measurement of radial mass density values on the Earth's radial scale.

Furthermore, Bangs, et al. [16] presented evidence that sinking seamounts may provide clues regarding slow-motion earthquake characteristics. Voisey, et al. [17] discussed the influence of the Earth's atmosphere and environmental factors on geological processes. The study also considered the influence of chemical changes associated with earthquakes. In addition, electricity generated during earthquakes may contribute to the formation of giant gold nuggets. The efficacy of China's clean-air actions in reducing pollution between 2013 and 2020 is discussed in Geng, et al. [18]. Cheesman, et al. [19] investigated reduced productivity and carbon drawdown in tropical forests caused by ground-level ozone exposure. Evidence for subsea permafrost in subarctic Canada linked to submarine groundwater discharge is presented in Normandeau, et al. [20].

Interesting discussions regarding tilted transverse isotropy in the Earth's inner core and the core–mantle boundary are presented in Brett, et al. [21]. Discussions regarding improvements in earthquake prediction accuracy can be found in Yavas, et al. [22]. Yang, et al. [23] presented the recognition of oil and gas reservoir structures based on deep learning methods. An interesting discussion on early peak ground acceleration prediction for on-site earthquake early warning using LSTM neural networks is presented in Hsu and Pratomo [24]. Cao, et

al. [25] discussed long short-term memory networks for pattern recognition in synthetically complete earthquake catalogs. LSTM-based deep learning methods for earthquake prediction using ionospheric data are discussed in [26]. Modernized *k-nearest* neighbors methods are presented in Yancey, et al. [27].

The application of neural networks to seismological prediction methods is presented in Wang, et al. [28]. Earthquake prediction using an evidential reasoning approach is discussed in Akter [29], while in the reference [30], the earthquake catalog of the National Observatory of Athens is discussed. A multi-task encoder–decoder framework for separating earthquake and ambient noise signals in seismograms is discussed in Yin, et al. [31]. Furthermore, a hybrid machine-learning model for estimating potential debris-flow volumes is presented in Huang, et al. [32]. This is followed by a discussion of earthquake perturbation identification using deep learning networks [33]. Zhang, et al. [34] presented a real-time automatic method for target localization under unknown wall characteristics in through-wall imaging. Ensemble learning using stochastic configuration networks for noisy optical fiber vibration signal recognition is discussed in Qu, et al. [35].

Furthermore, Rawat, et al. [36] discussed whether site-specific parameters can help identify seismically induced damage patterns. This is followed by a discussion of seismic discrimination between nuclear explosions and natural earthquakes using multi-machine-learning techniques in Elkhoully and Ali [37]. A significant limitation in applying conventional fuzzy theory to earthquake prediction is the exponential growth in the number of rules as the number of variables increases. This problem is addressed here through the introduction of a non-conventional analytical method for earthquake prediction. For this purpose, a new adaptive analytical function is defined to determine the positions of the centers of the output fuzzy sets instead of relying on a conventional fuzzy rule base [38]. Finally, Buckreis, et al. [39] applied fuzzy logic theory and artificial intelligence methods to earthquake prediction.

2. Dynamics of Earthquakes in Radial Mass Density Theory

In this study, a new Relativistic Radial Density Theory (RRDT) [15] is applied as a theoretical framework for analyzing energy-density variations in the Earth, with potential relevance to seismic processes. Since the value of the cosmological constant Λ has 3 values, in the presented theory, it is introduced a new energy conservation constant \mathcal{K} . To do it, one can start with the Planck mass, M_p , and Planck length, L_p .

$$L_p = \frac{2GM_p}{(1+\kappa)c^2}, \quad \kappa = \frac{2GM_p}{L_p c^2} - 1 = 0.99993392118. \quad (1)$$

Using (1), we can calculate the maximal radial mass density value ρ_{rmax} .

$$\rho_{rmax} = \frac{M_p}{r_{pmin}} = \frac{M_g}{r_{gmin}} = \frac{(1+\kappa)c^2}{G},$$

$$\rho_{rmax} = 2.693182 \cdot 10^{27} \text{ kg / m}, \quad (2)$$

Here, M_g and r_g are the gravitational mass and radius, respectively. On the other hand, the minimal radial mass density value, ρ_{rmin} , can be obtained by using the following relations:

$$\rho_{rmin} = \frac{M_p}{r_{pmax}} = \frac{M_g}{r_{gmax}} = \frac{(1-\kappa)c^2}{G},$$

$$\rho_{rmin} = 0.888779 \cdot 10^{23} \text{ kg / m}. \quad (3)$$

Since the maximal Earth radius is not known here, a parameter x is introduced in order to calculate the maximal Earth radius (r_{max}) and the related new Earth mass, M_{new} .

$$r_{max} = x \cdot r_{present} = x \cdot 6371 \cdot 10^3 \text{ m},$$

$$M_{new} = \rho_{rmin} r_{max} = x \cdot 5.662411 \cdot 10^{29} \text{ kg}. \quad (4)$$

Now, following of the new Earth mass, one can calculate the related minimal and maximal Earth radii.

$$r_{emin} = \frac{M_{new}}{\rho_{rmax}} = x \cdot 2.102509 \cdot 10^2 \text{ m},$$

$$r_{emax} = \frac{M_{new}}{\rho_{rmin}} = x \cdot 6371,033744 \cdot 10^3 \text{ m}. \quad (5)$$

Further, one can calculate the minimal and the maximal Earth's radii as a function of the energy conservation constant \mathcal{K} .

$$r_{emin} = \frac{GM_{new}}{(1+\kappa)}, \quad r_{emax} = \frac{GM_{new}}{(1-\kappa)}. \quad (6)$$

The related ratio of the maximal and the minimal gravitational radii is given by the relation.:

$$\frac{r_{emax}}{r_{emin}} = \frac{(1+\kappa)}{(1-\kappa)} = 30,265.847623. \quad (7)$$

Now, the ratio, R , between official Earth mass, M_{off} , and calculated new Earth mass, M_{new} , has been given by the relation.

$$R_e = \frac{M_{e\text{off}} \cdot 100}{M_{e\text{new}}} = \frac{5.97219 \cdot 10^{24} \cdot 100}{x \cdot 5.662411 \cdot 10^{29}} = \frac{1}{x} 0.001054\% \tag{8}$$

To solve the problem of the earthquake measurement on the radial mass density scale, one can start with the inclusion of the following parameters.

$$r_{N_i} = N_i n_i r_{\min}, \quad N_i = 1, 2, \dots, N_{\max},$$

$$\text{for } n_i = 1, 2, \dots, n_{i\max}. \tag{9}$$

Here, parameter n_i denotes the first position of the measurement instrument on the Earth's radial scale. The radial positions of the other measurement instruments are defined by r_{N_i} , where $i=1, 2, \dots, i_{\max}$. The measurement instruments should give (among others) the related amplitudes of the earthquake signals. In that way, one can connect the positions of the instruments by the related radial mass density value, ρ_{rr} (4). Including the radial positions of the earthquake's instruments (9) into the relations of the potential forces F_{p_x} , F_{p_y} , and F_{p_z} one obtains the new form of these forces:

$$F_{N_i p_x} = \frac{\partial}{\partial x} qV_{N_i e} + \frac{\partial}{\partial x} m_{N_i} \left(-G\rho_{r\max} r_{\min} / r_{N_i} \cos \theta_{N_i} \right),$$

$$F_{N_i p_y} = \frac{\partial}{\partial y} qV_{N_i e} + \frac{\partial}{\partial y} m_{N_i} \left(-G\rho_{r\max} r_{\min} / r_{N_i} \cos \theta_{N_i} \right),$$

$$F_{N_i p_z} = \frac{\partial}{\partial z} qV_{N_i e} + \frac{\partial}{\partial z} m_{N_i} \left(-G\rho_{r\max} r_{\min} / r_{N_i} \cos \theta_{N_i} \right). \tag{10}$$

Here, q is the elementary electric charge, $V_{N_i e}$ is a scalar potential of the electromagnetic field, and m_{N_i} is the mass of the i -th earthquake's measurement instrument. Thus, the positions of the earthquake measurement instruments are given by the relations:

$$r_1 = n_{\text{inst}1} r_{\min}, r_2 = n_{\text{inst}2} r_{\min}, \dots, r_{N_i} = n_{\max} r_{\min}. \tag{11}$$

Now, following the practical point of view, the second possibility of the description of the positions of the earthquake measurement instruments is to start with the maximum Earth's radius. Thus, in that case, the first earthquake measurement instrument layer can be on the Earth's surface. Let the radial distance between the earthquake's instruments (sensors) is d , in meters. In that case, the radial positions of the earthquake sensors can be described by the relations:

$$r_1 = r_{e\max}, \quad r_2 = r_{e\max} - d, \quad r_k = r_{e\max} - kd,$$

$$k = 1, 2, \dots, k_{\max}, \quad \text{for } d = 50m,$$

$$r_2 = r_{e\max} - 50, \quad r_k = r_{e\max} - 50k. \tag{12}$$

The distance between the earthquake measurement instruments, d , and the maximum number of the earthquake instruments, k_{\max} , are functions of the Earth's structure in the related region. Starting with the minimal radial mass density value, $\rho_{r\min}$, the earthquake's dynamics can now be described as the functions of the potentials p_x, p_y, p_z .

$$p_x = M_{e\text{new}} v_x = \rho_{r\min} r_{e\max} v_x,$$

$$p_y = M_{e\text{new}} v_y = \rho_{r\min} r_{e\max} v_y,$$

$$p_z = M_{e\text{new}} v_z = \rho_{r\min} r_{e\max} v_z. \tag{13}$$

Here, v_x, v_y and v_z are related velocities in x, y , and z directions. Finally, one can define the potential forces $F_{p_x}, F_{p_y}, F_{p_z}$ as the functions of the total potential energy and minimal radial mass density in the potential field.

$$F_{p_x} = -\frac{\partial U}{\partial x} = \frac{\partial}{\partial x} qV_e + \frac{\partial}{\partial x} m_i \left(-G\rho_{r\min} r_{\max} / r \right),$$

$$F_{p_y} = -\frac{\partial U}{\partial y} = \frac{\partial}{\partial y} qV_e + \frac{\partial}{\partial y} m_i \left(-G\rho_{r\min} r_{\max} / r \right),$$

$$F_{p_z} = -\frac{\partial U}{\partial z} = \frac{\partial}{\partial z} qV_e + \frac{\partial}{\partial z} m_i \left(-G\rho_{r\min} r_{\max} / r \right). \tag{14}$$

Now, if the earthquake had happened at the determined region, the Earth's radius would have the new value r_N . In that case, the relations in (14) can be transformed into the new form.

$$F_{p_x} = -\frac{\partial U_{Ne}}{\partial x} = \frac{\partial}{\partial x} qV_{Ne} + \frac{\partial}{\partial x} m_i \left(-G\rho_{r\min} r_{\max} / r_N \right),$$

$$F_{p_y} = -\frac{\partial U_{Ne}}{\partial y} = \frac{\partial}{\partial y} qV_{Ne} + \frac{\partial}{\partial y} m_i \left(-G\rho_{r\min} r_{\max} / r_N \right),$$

$$F_{p_z} = -\frac{\partial U_{Ne}}{\partial z} = \frac{\partial}{\partial z} qV_{Ne} + \frac{\partial}{\partial z} m_i \left(-G\rho_{r\min} r_{\max} / r_N \right). \tag{15}$$

In the case where the earthquake is not in the radial direction, one should include the related projection to the radial coordinates.

$$\begin{aligned}
 F_{Np_x} &= -\frac{\partial U_N}{\partial x} = \frac{\partial}{\partial x} qV_{Ne} + \frac{\partial}{\partial x} m_i \left(-G\rho_{r_{min}} r_{max} / r_N \cos\theta_x \right), \\
 F_{Np_y} &= -\frac{\partial U_N}{\partial y} = \frac{\partial}{\partial y} qV_{Ne} + \frac{\partial}{\partial y} m_i \left(-G\rho_{r_{min}} r_{max} / r_N \cos\theta_y \right), \\
 F_{Np_z} &= -\frac{\partial U_N}{\partial z} = \frac{\partial}{\partial z} qV_{Ne} + \frac{\partial}{\partial z} m_i \left(-G\rho_{r_{min}} r_{max} / r_N \cos\theta_z \right).
 \end{aligned} \tag{16}$$

Here parameters, θ_x , θ_y , and θ_z are the angles between the radial direction and coordinates x , y , and z , respectively.

To solve the problem of the earthquake measurement on the radial mass density scale (starting with the position at the minimal Earth radius), one can use the following relations.

$$\begin{aligned}
 r_{N_i} &= N_i n_i r_{min}, \quad N_i = 1, 2, \dots, N_{max}, \quad \text{for } i = 1, \quad N_1 = 1, \\
 \text{and } n_1 &= 10, \quad r_{N_1} = 1 * 10 * 2, 1 * 10^2 m = 2, 1 \text{ km}.
 \end{aligned} \tag{17}$$

Here parameter r_{N_i} denotes the first position of the measurement instrument on the radial scale. The positions of the other measurement instruments are denoted by r_{n_i} , where $i = 1, 2, \dots, i_{max}$. The measurement instruments should predict the related place, time, and amplitude of future earthquakes. The positions of the measurement instruments with the maximal radial mass density value, $\rho_{r_{max}}$, are given in (2).

Now, including the positions of the earthquake measurement instruments (16) and (17) into the relations of the potential forces F_{p_x} , F_{p_y} , and F_{p_z} (15), one obtains the new form of these forces:

$$\begin{aligned}
 F_{N_i p_x} &= \frac{\partial}{\partial x} qV_{N_i e} + \frac{\partial}{\partial x} m \left(-G\rho_{r_{max}} r_{min} / r_{N_i} \cos\theta_{N_i} \right), \\
 F_{N_i p_y} &= \frac{\partial}{\partial y} qV_{N_i e} + \frac{\partial}{\partial y} m \left(-G\rho_{r_{max}} r_{min} / r_{N_i} \cos\theta_{N_i} \right), \\
 F_{N_i p_z} &= \frac{\partial}{\partial z} qV_{N_i e} + \frac{\partial}{\partial z} m \left(-G\rho_{r_{max}} r_{min} / r_{N_i} \cos\theta_{N_i} \right).
 \end{aligned} \tag{18}$$

Generally, the positions of the earthquake measurement instruments can be determined by the following relations:

$$r_1 = n_1 r_{min}, \quad r_2 = 2n_1 r_{min}, \dots, r_{N_i} = N_i n_1 r_{min}. \tag{19}$$

From a practical perspective, the positions of earthquake measurement instruments can be determined starting from the position of the maximum (today's) Earth radius. Let the first earthquake measurement instrument be on the Earth's surface. Furthermore, let the radial distance between the two earthquake measurement instruments be equal to d in meters. The following relations can then be used to determine the positions of the earthquake measurement instruments.

$$\begin{aligned}
 r_1 &= r_{max} = r_{Earth}, \quad r_2 = r_{Earth} - d, \\
 r_k &= r_{Earth} - kd, \quad k = 1, 2, \dots, k_{max}.
 \end{aligned} \tag{20}$$

In the general point of view, the distance between two earthquake measurement instruments, d , and the maximum number of earthquake measurement instruments, k , depend on the Earth's structure in the related regions. Earthquake dynamics can now be described starting with the minimal radial mass density value at the maximum radius.

$$\begin{aligned}
 M_{earth} &= \rho_{r_{min}} r_{earth} = const., \quad r = \rho_{r_{min}} r_{earth} / \rho_r, \\
 p_x &= M_{earth} v_x = \rho_{r_{min}} r_{earth} v_x, \quad p_y = M_{earth} v_y = \rho_{r_{min}} r_{earth} v_y, \\
 p_z &= M_{earth} v_z = \rho_{r_{min}} r_{earth} v_z.
 \end{aligned} \tag{21}$$

Here M_{earth} is the Earth mass, and p_x , p_y and p_z are related potentials. Finally, one can define the potential forces F_{p_x} , F_{p_y} , F_{p_z} as the function of the total potential energy and minimal radial mass density in the multi-potential field.

$$\begin{aligned}
 F_{p_x} &= -\frac{\partial U}{\partial x} = \frac{\partial}{\partial x} qV_e + \frac{\partial}{\partial x} m_i \left(-G\rho_{r_{min}} r_{max} / r \right), \\
 F_{p_y} &= -\frac{\partial U}{\partial y} = \frac{\partial}{\partial y} qV_e + \frac{\partial}{\partial y} m_i \left(-G\rho_{r_{min}} r_{max} / r \right), \\
 F_{p_z} &= -\frac{\partial U}{\partial z} = \frac{\partial}{\partial z} qV_e + \frac{\partial}{\partial z} m_i \left(-G\rho_{r_{min}} r_{max} / r \right).
 \end{aligned} \tag{22}$$

For the measurement of the earthquake signals, the potential forces should also be functions of the electrical potential V_e . In that case, one can use the earthquake measurement instruments, which also include the electrical field. After the radial density, ρ_r , was changed at some determined region, the related Earth radius obtains a new value, r_{new} . In that case, the relations in (22) can be transformed into the new form.

$$\begin{aligned}
 F_{p_x} &= -\frac{\partial U_{new}}{\partial x} = \frac{\partial}{\partial x} qV_{Ne} + \frac{\partial}{\partial x} m_i \left(-G\rho_{r_{min}} r_{max} / r_{new} \right), \\
 F_{p_y} &= -\frac{\partial U}{\partial y} = \frac{\partial}{\partial y} qV_{Ne} + \frac{\partial}{\partial y} m_i \left(-G\rho_{r_{min}} r_{max} / r_{new} \right), \\
 F_{p_z} &= -\frac{\partial U}{\partial z} = \frac{\partial}{\partial z} qV_{Ne} + \frac{\partial}{\partial z} m_i \left(-G\rho_{r_{min}} r_{max} / r_{new} \right).
 \end{aligned} \tag{23}$$

In the case where the earthquake is not in the radial direction, one can include the related projection to the radial coordinates.

$$\begin{aligned}
 F_{Np_x} &= -\frac{\partial U_N}{\partial x} = \frac{\partial}{\partial x} qV_{Ne} + \frac{\partial}{\partial x} m_i (-G\rho_{r_{min}} r_{max} / r_N \cos \theta_x), \\
 F_{Np_y} &= -\frac{\partial U_N}{\partial y} = \frac{\partial}{\partial y} qV_{Ne} + \frac{\partial}{\partial y} m_i (-G\rho_{r_{min}} r_{max} / r_N \cos \theta_y), \\
 F_{Np_z} &= -\frac{\partial U_N}{\partial z} = \frac{\partial}{\partial z} qV_{Ne} + \frac{\partial}{\partial z} m_i (-G\rho_{r_{min}} r_{max} / r_N \cos \theta_z).
 \end{aligned}
 \tag{24}$$

Here, parameters, $\cos(\theta_x)$, $\cos(\theta_y)$, and $\cos(\theta_z)$ give the projections of the earthquake direction on the x , y , and z axes.

Intensity of the earthquakes is measured by the seismometers, which are presented as the earthquake magnitude. Therefore, it is of interest to connect the radial mass density value, ρ_r , with the earthquake magnitude M_s . The maximal and minimal radial mass density in the gravitational field are equal to:

$$\begin{aligned}
 \rho_{rmax} &= 2.693182 \cdot 10^{27} \text{ kg / m}, \\
 \rho_{rmin} &= 0.888779 \cdot 10^{23} \text{ kg / m}.
 \end{aligned}
 \tag{25}$$

Further, one can connect the earthquake magnitudes with the radial mass density, ρ_{rm} .

$$M_s = f(M_{earth} / r) = f \cdot \rho_{rm}.
 \tag{26}$$

Here, parameter f is the conversion factor between the earthquake magnitude and the radial mass density. This parameter should be estimated by using the related experiments.

To reduce the number of required measurement instruments within a region of interest, the use of mobile robotic platforms can be considered. Such systems offer greater flexibility compared to conventional static monitoring stations. In particular, mobile platforms can be equipped with multiple sensing modalities, including seismographic instruments, as well as additional sensors capable of capturing quantities relevant to the proposed framework, such as proxies for radial mass–energy density variations and other geophysically relevant parameters.

An important advantage of this approach lies in the ability to perform spatially adaptive measurements, enabling more efficient data acquisition across heterogeneous regions. Additionally, the deployment of mobile systems may contribute to cost reduction by optimizing sensor coverage and reducing the need for dense networks of fixed instruments. Such capabilities are particularly relevant for exploring spatial and temporal variations predicted by the proposed theoretical framework.

3. Conclusion

This study presents a theoretical framework for analyzing radial mass–energy density distributions in geophysical systems, based on the Relativistic Radial Density Theory (RRDT). By introducing an energy-based formalism grounded in fundamental physical considerations, the model provides a structured framework for describing spatial and temporal variations in radial density fields and their possible relation to large-scale geophysical dynamics.

The contribution of this work lies in proposing a novel theoretical perspective that may stimulate interdisciplinary research at the interface of physics, geophysics, and systems science, and in outlining a possible pathway toward its future experimental assessment. The proposed approach should be interpreted as a conceptual and exploratory model. In this sense, the framework may serve as a basis for formulating testable hypotheses regarding the role of density perturbations in lithospheric processes.

At the same time, the present formulation relies on simplifying assumptions and has not yet been empirically validated. Future work should therefore focus on establishing quantitative links between measurable physical quantities and the theoretical variables introduced in this study. This includes the development of appropriate sensing methodologies, the calibration of model parameters, and the validation of the framework using observational data and numerical simulations. Additionally, further theoretical work is required to connect the proposed formulation with established models in continuum mechanics, geophysics, and complex systems theory.

References

- [1] S. E. Hough and M. Page, "A century of induced earthquakes in Oklahoma?," *Bulletin of the Seismological Society of America*, vol. 105, no. 6, pp. 2863-2870, 2015.
- [2] R. Okuwaki, Y. Yagi, T. Taymaz, and S. P. Hicks, "Seismological analysis of the two earthquakes that devastated southern Turkey," *Phys.org (News Article Reporting University of Tsukuba Research Based on Geophysical Research Letters)*, 2023.
- [3] H. Shiraishi, "Earthquake prediction software on global scale," *Journal of Geoscience and Environment Protection*, vol. 10, no. 3, pp. 34-45, 2022. <https://doi.org/10.4236/gep.2022.103003>
- [4] C. Fliedner and M. E. French, "Measurements of wave-induced attenuation in saturated metapelite and the band-limitation of low-frequency earthquakes," *AGU Advances*, vol. 4, no. 2, p. e2022AV000837, 2023. <https://doi.org/10.1029/2022AV000837>
- [5] F. Freund, "Toward a unified solid state theory for pre-earthquake signals," *Acta Geophysica*, vol. 58, no. 5, pp. 719-766, 2010. <https://doi.org/10.2478/s11600-009-0066-x>
- [6] C. G. Sammis and M. G. Bostock, "A granular jamming model for low-frequency earthquakes," *Journal of Geophysical Research: Solid Earth*, vol. 126, no. 7, p. e2021JB021963, 2021. <https://doi.org/10.1029/2021JB021963>
- [7] Z. Qu, F. Wang, X. Chen, X. Wang, and Z. Zhou, "Rapid report of seismic damage to hospitals in the 2023 Turkey earthquake sequences," *Earthquake Research Advances*, vol. 3, no. 4, p. 100234, 2023. <https://doi.org/10.1016/j.eqrea.2023.100234>
- [8] A. Burnol *et al.*, "Impacts of water and stress transfers from ground surface on the shallow earthquake of 11 November 2019 at Le Teil (France)," *Remote Sensing*, vol. 15, no. 9, p. 2270, 2023. <https://doi.org/10.3390/rs15092270>
- [9] S.-R. G. Christopoulos, E. S. Skordas, and N. V. Sarlis, "On the statistical significance of the variability minima of the order parameter of seismicity by means of event coincidence analysis," *Applied Sciences*, vol. 10, no. 2, p. 662, 2020. <https://doi.org/10.3390/app10020662>
- [10] G. Farge, N. M. Shapiro, and W. B. Frank, "Moment-duration scaling of low-frequency earthquakes in Guerrero, Mexico," *Journal of Geophysical Research: Solid Earth*, vol. 125, no. 8, p. e2019JB019099, 2020. <https://doi.org/10.1029/2019JB019099>
- [11] D. S. Helman, "Seismic electric signals (SES) and earthquakes: A review of an updated VAN method and competing hypotheses for SES generation and earthquake triggering," *Physics of the Earth and Planetary Interiors*, vol. 302, p. 106484, 2020. <https://doi.org/10.1016/j.pepi.2020.106484>

- [12] C. F. Richter, "An instrumental earthquake magnitude scale," *Bulletin of the Seismological Society of America*, vol. 25, no. 1, pp. 1–32, 1935. <https://doi.org/10.1785/BSSA0250010001>
- [13] G. Mercalli, "On the proposed modifications to the De Rossi-Forel seismic scale," *Bollettino della Società Sismologica Italiana*, vol. 8, pp. 184–191, 1902.
- [14] H. O. Wood and F. Neumann, "Modified Mercalli intensity scale of 1931," *Bulletin of the Seismological Society of America*, vol. 21, no. 4, pp. 277–283, 1931. <https://doi.org/10.1785/BSSA0210040277>
- [15] B. Novakovic, "Relativistic radial density theory (RRDT)," *Universal Journal of Physics Research*, vol. 1, no. 1, pp. 77–87, 2022. <https://doi.org/10.31586/ujpr.2022.500>
- [16] N. L. Bangs *et al.*, "Slow slip along the Hikurangi margin linked to fluid-rich sediments trailing subducting seamounts," *Nature Geoscience*, vol. 16, no. 6, pp. 505–512, 2023. <https://doi.org/10.1038/s41561-023-01186-3>
- [17] C. R. Voisey *et al.*, "Gold nugget formation from earthquake-induced piezoelectricity in quartz," *Nature Geoscience*, vol. 17, no. 9, pp. 920–925, 2024. <https://doi.org/10.1038/s41561-024-01514-1>
- [18] G. Geng *et al.*, "Efficacy of China's clean air actions to tackle PM_{2.5} pollution between 2013 and 2020," *Nature Geoscience*, vol. 17, no. 10, pp. 987–994, 2024. <https://doi.org/10.1038/s41561-024-01540-z>
- [19] A. W. Cheesman *et al.*, "Reduced productivity and carbon drawdown of tropical forests from ground-level ozone exposure," *Nature Geoscience*, vol. 17, no. 10, pp. 1003–1007, 2024. <https://doi.org/10.1038/s41561-024-01530-1>
- [20] A. Normandeau *et al.*, "Evidence for subsea permafrost in subarctic Canada linked to submarine groundwater discharge," *Nature Geoscience*, vol. 17, no. 10, pp. 1022–1030, 2024. <https://doi.org/10.1038/s41561-024-01497-z>
- [21] H. Brett, J. Tromp, and A. Deuss, "Tilted transverse isotropy in earth's inner core," *Nature Geoscience*, vol. 17, no. 10, pp. 1059–1064, 2024. <https://doi.org/10.1038/s41561-024-01539-6>
- [22] C. E. Yavas, L. Chen, C. Kadlec, and Y. Ji, "Improving earthquake prediction accuracy in Los Angeles with machine learning," *Scientific Reports*, vol. 14, p. 24440, 2024.
- [23] S. Yang, A. Jin, and Y. Xu, "Recognition of oil and gas reservoir space based on deep learning," *E3S Web of Conferences*, vol. 267, p. 01038, 2021. <https://doi.org/10.1051/e3sconf/202126701038>
- [24] T.-Y. Hsu and A. Pratomo, "Early peak ground acceleration prediction for on-site earthquake early warning using LSTM neural network," *Frontiers in Earth Science*, vol. 10, p. 911947, 2022. <https://doi.org/10.3389/feart.2022.911947>
- [25] C. Cao *et al.*, "Long short-term memory networks for pattern recognition of synthetical complete earthquake catalog," *Sustainability*, vol. 13, no. 9, p. 4905, 2021. <https://doi.org/10.3390/su13094905>
- [26] R. Abri and H. Artuner, "LSTM-based deep learning methods for prediction of earthquakes using ionospheric data," *Gazi University Journal of Science*, vol. 35, no. 4, pp. 1417–1431, 2022. <https://doi.org/10.35378/gujs.950387>
- [27] R. E. Yancey, B. Xin, and N. Matloff, "Modernizing k-nearest neighbors," *Stat*, vol. 10, no. 1, p. e335, 2021. <https://doi.org/10.1002/sta4.335>
- [28] W. Wang, G.-F. Wu, and X.-Y. Song, "The application of neural networks to comprehensive prediction by seismology prediction method," *Acta Seismologica Sinica*, vol. 13, no. 2, pp. 210–215, 2000. <https://doi.org/10.1007/s11589-000-0012-0>
- [29] S. Akter, M. J. A. Patwary, and S. Hossain, "Earthquake prediction by using evidential reasoning approach," *International Journal of Research in Engineering and Technology*, vol. 4, no. 12, pp. 149–151, 2015.
- [30] G. Chouliaras, "Investigating the earthquake catalog of the National Observatory of Athens," *Natural Hazards and Earth System Sciences*, vol. 9, no. 3, pp. 905–912, 2009. <https://doi.org/10.5194/nhess-9-905-2009>
- [31] J. Yin, M. A. Denolle, and B. He, "A multitask encoder–decoder to separate earthquake and ambient noise signal in seismograms," *Geophysical Journal International*, vol. 231, no. 3, pp. 1806–1822, 2022. <https://doi.org/10.1093/gji/ggac290>
- [32] J. Huang, T. C. Hales, R. Huang, N. Ju, Q. Li, and Y. Huang, "A hybrid machine-learning model to estimate potential debris-flow volumes," *Geomorphology*, vol. 367, p. 107333, 2020. <https://doi.org/10.1016/j.geomorph.2020.107333>
- [33] P. Xiong, D. Marchetti, A. De Santis, X. Zhang, and X. Shen, "SafeNet: SwArm for earthquake perturbations identification using deep learning networks," *Remote Sensing*, vol. 13, no. 24, p. 5033, 2021. <https://doi.org/10.3390/rs13245033>
- [34] H.-M. Zhang, S. Zhou, C. Xu, and Y.-R. Zhang, "A real-time automatic method for target locating under unknown wall characteristics in through-wall imaging," *Progress In Electromagnetics Research M*, vol. 89, pp. 189–197, 2020. <https://doi.org/10.2528/PIERM19111101>
- [35] H. Qu, T. Feng, Y. Zhang, and Y. Wang, "Ensemble learning with stochastic configuration network for noisy optical fiber vibration signal recognition," *Sensors*, vol. 19, no. 15, p. 3293, 2019. <https://doi.org/10.3390/s19153293>
- [36] A. Rawat, R. S. Chatterjee, D. Kumar, H. Kumar, and S. Suman, "Can site specific parameters help to identify the seismically induced damage pattern: An assessment," *Research Square*, 2023. <https://doi.org/10.21203/rs.3.rs-2721236/v1>
- [37] S. H. Elkhoully and G. Ali, "Seismic discrimination between nuclear explosions and natural earthquakes using multi-machine learning techniques," *Pure and Applied Geophysics*, vol. 182, pp. 4879–4890, 2025. <https://doi.org/10.1007/s00024-024-03463-7>
- [38] B. M. Novakovic, "Fuzzy logic control synthesis without any rule base," *IEEE Transactions on Systems, Man, and Cybernetics, Part B (Cybernetics)*, vol. 29, no. 3, pp. 459–466, 1999. <https://doi.org/10.1109/3477.764883>
- [39] T. E. Buckreis *et al.*, "Engineering attributes of ground motions from February 2023 Türkiye earthquake sequence," *Earthquake Spectra*, vol. 40, no. 4, pp. 2268–2284, 2024. <https://doi.org/10.1177/87552930241259024>